

# Ambient ultrafine particles alter lipid metabolism and HDL anti-oxidant capacity in LDLR-null mice<sup>§</sup>

Rongsong Li,<sup>\*,†</sup> Mohamad Navab,<sup>†</sup> Payam Pakbin,<sup>§</sup> Zhi Ning,<sup>\*\*</sup> Kaveh Navab,<sup>†</sup> Greg Hough,<sup>†</sup> Todd E. Morgan,<sup>††</sup> Caleb E. Finch,<sup>††</sup> Jesus A. Araujo,<sup>†</sup> Alan M. Fogelman,<sup>†</sup> Constantinos Sioutas,<sup>§</sup> and Tzung Hsiai<sup>1,\*†</sup>

Department of Biomedical Engineering,\* Department of Civil Engineering and Environmental Science,<sup>§</sup> and Davis School of Gerontology,<sup>††</sup> University of Southern California, Los Angeles, CA; Division of Cardiology,<sup>†</sup> Department of Medicine, University of California, Los Angeles School of Medicine, Los Angeles, CA; and School of Energy and Environment,<sup>\*\*</sup> City University of Hong Kong, Hong Kong

**Abstract** Exposure to ambient particulate matter (PM) is a risk factor for cardiovascular diseases. The redox-active ultrafine particles (UFPs) promote vascular oxidative stress and inflammatory responses. We hypothesized that UFPs modulated lipid metabolism and anti-oxidant capacity of high density lipoprotein (HDL) with an implication in atherosclerotic lesion size. Fat-fed low density lipoprotein receptor-null (LDLR<sup>-/-</sup>) mice were exposed to filtered air (FA) or UFPs for 10 weeks with or without administering an apolipoprotein A-I mimetic peptide made of D-amino acids, D-4F. LDLR<sup>-/-</sup> mice exposed to UFPs developed a reduced plasma HDL level ( $P < 0.01$ ), paraoxonase activity ( $P < 0.01$ ), and HDL anti-oxidant capacity ( $P < 0.05$ ); but increased LDL oxidation, free oxidized fatty acids, triglycerides, serum amyloid A ( $P < 0.05$ ), and tumor necrosis factor  $\alpha$  ( $P < 0.05$ ), accompanied by a 62% increase in the atherosclerotic lesion ratio of the en face aortic staining and a 220% increase in the cross-sectional lesion area of the aortic sinus ( $P < 0.001$ ). D-4F administration significantly attenuated these changes. UFP exposure promoted pro-atherogenic lipid metabolism and reduced HDL anti-oxidant capacity in fat-fed LDLR<sup>-/-</sup> mice, associated with a greater atherosclerotic lesion size compared with FA-exposed animals. D-4F attenuated UFP-mediated pro-atherogenic effects, suggesting the role of lipid oxidation underlying UFP-mediated atherosclerosis.—Li, R., M. Navab, P. Pakbin, Z. Ning, K. Navab, G. Hough, T. E. Morgan, C. E. Finch, J. A. Araujo, A. M. Fogelman, C. Sioutas, and T. Hsiai. **Ambient ultrafine particles alter lipid metabolism and HDL anti-oxidant capacity in LDLR-null mice.** *J. Lipid Res.* 2013. 54: 1608–1615.

**Supplementary key words** atherosclerosis • D-4F • low density lipoprotein receptor-null • high density lipoprotein

This project was supported by National Institutes of Health Grants R01HL-083015 (T.K.H.), R21HL-091302 (T.K.H.), and P0HL-030568 (A.M.F.). The Southern California Particle Center was funded by the Environmental Protection Agency Science to Achieve Results (EPA STAR) program [award number 2145 G GB139 (C.S.)], South Coast Air Quality Management District [award number 11527 (C.S.)], and National Institute of Environmental Health Sciences Grant R01ES-016959 (J.A.A.). Both Dr. Alan M. Fogelman and Dr. Mohamad Navab hold a patent on D-4F at University of California, Los Angeles.

Manuscript received 14 December 2012 and in revised form 21 March 2013.

Published, JLR Papers in Press, April 6, 2013  
DOI 10.1194/jlr.M035014

Exposure to ambient particulate matter (PM) is deemed as a modifiable risk factor to cardiovascular morbidity and mortality (1–3). While epidemiological studies support the atherogenic effects of PM, the ultrafine particles (UFPs) ( $d_p < 100\text{--}200$  nm), highly enriched in redox-active cycling organic chemicals (4), engender higher pro-oxidizing potential than those of large particles (5, 6). These ambient UFPs reduce anti-inflammatory capacity of high density lipoprotein (HDL), and enhance atherosclerosis (7). However, the role of lipid metabolism and HDL function in UFP-mediated atherosclerotic lesions remained to be explored.

HDL has both anti-oxidant and anti-inflammatory capacities to provide atheroprotective mechanisms (8, 9). In patients with systemic inflammation such as atherosclerosis, metabolic syndromes, and chronic renal disease, HDL is dysfunctional and pro-inflammatory (10, 11), and both apolipoprotein A-I (ApoA-I) and paraoxonase (PON) levels and activities were reduced (10–12). D-4F, an ApoA-I mimetic peptide made of D-amino acids, restored HDL function and attenuated atherosclerosis in ApoE-null mice (13, 14). Hence, administration of D-4F may provide a basis to elucidate lipid metabolism and HDL dysfunction underlying UFP-mediated atherosclerosis.

For these reasons, we hypothesized that UFP exposure promoted atherosclerotic lesion size by modulating lipid

Abbreviations: DCF, dichlorofluorescein; D-4F, mimetic peptide of apolipoprotein A-I made of D-amino acids; 14-15EET, 14(15)-epoxy-5Z,8Z,11Z-eicosatrienoic acid; FA, filtered air; HETE, hydroxyeicosatetraenoic acid; HFD, high-fat diet; HODE, hydroxyoctadecadienoic acid; HOI, HDL oxidation index; LDLR<sup>-/-</sup>, low density lipoprotein receptor-null; PGD2, prostaglandin D2; PGE2, prostaglandin E2; PM, particulate matter; PON, paraoxonase; SAA, serum amyloid A; TNF- $\alpha$ , tumor necrosis factor  $\alpha$ ; TXB2, thromboxane; UFP, ultrafine particle; USC, University of Southern California.

<sup>1</sup>To whom correspondence should be addressed.

e-mail: hsiai@usc.edu

<sup>§</sup>The online version of this article (available at <http://www.jlr.org>) contains supplementary data in the form of text, six figures, and four tables.

metabolism and reducing HDL anti-oxidant capacity. Low density lipoprotein receptor-null (LDLR<sup>-/-</sup>) mice fed on a high-fat diet (HFD) were exposed to filtered air (FA) versus UFPs collected near downtown Los Angeles in the presence or absence of D-4F administration. We quantified HDL anti-oxidant capacity, PON activity, serum amyloid A (SAA) and tumor necrosis factor  $\alpha$  (TNF- $\alpha$ ) levels, plasma lipid profiles, LDL oxidation, and oxidative products of arachidonic and linoleic acids, namely, hydroxyicosatetraenoic acids (HETEs) and hydroxyoctadecadienoic acids (HODEs), in relation to the atherosclerotic lesion size. D-4F was administered to elucidate the role of plasma lipoproteins and HDL functionality underlying UFP-induced atherosclerosis.

## MATERIALS AND METHODS

### UFP collections and sample preparation

The collection of the UFPs was conducted at the University of Southern California (USC) campus located in the urban regions of Los Angeles, in close proximity to a network of major freeways. These aerosols represent a mixture of pollution sources, including fresh ambient PM from areas impacted by heavy-duty diesel trucks and light-duty gasoline vehicles, as well as PM generated by photochemical oxidation of primary organic vapors. The USC site is representative of the numerous urban regions in the USA where high concentrations of PM are freshly emitted from vehicular traffic on nearby freeways. UFP samples were collected by a high-volume particle sampler as previously described (15). The collected PM samples were extracted from the filter substrates, and were re-aerosolized for the exposure experiment as previously described (16). The size distribution of UFPs was comparable to the representative aerosols collected in downtown Los Angeles at the USC site (supplementary Fig. 1) as previously described (17). Chemical analysis was also performed on the UFPs (for details refer to Supplementary Methods). The chemical compositions of UFPs and the concentration (in terms of ratios in total PM) of the main chemical constituents of UFPs including inorganic ions; organic, elemental, and total carbon content; and selected redox-active metal species is presented in supplementary Table I and supplementary Fig. II.

### Mouse exposure to UFPs in the presence or absence of D-4F

All animal experiments were performed in the Vivarium in the Ray R. Irani Building in compliance with USC Institutional Animal Care and Use Committee protocol. Age-matched LDLR<sup>-/-</sup> male mice under the C57BL/6 background (stock number 002207, Jackson Laboratory) were exposed to UFPs or High-efficiency particulate air (HEPA)-FA (used as control group) via whole-body animal exposure chambers on a HFD (D12492: 5.24 kcal/g, 34.9 g% fat, 26.2 g% protein, 26.2 g% carbohydrate; Research Diets) starting at the age of 90 days. In reference to the previous exposure duration/dosage of exposure (7), the mice were exposed to UFPs at mass concentrations of approximately 360  $\mu\text{g}/\text{m}^3$  for 5 h per day and 3 days per week for 10 weeks (please see Supplementary Methods for details). During exposure, a scanning mobility particle sizer (SMPS Model 3080, TSI Inc.) was used, in parallel with the animal exposure chambers, to monitor particle sizes and concentrations.

D-4F was initially administered via subcutaneous injection at 0.2 mg/ml/mouse, and saline was injected as the control. After the first week, D-4F was administered via drinking water

at 0.2 mg/ml in response to death from subcutaneous injection. The averaged water consumption of mice was 4.03 ml per day. There was no significant difference in the weight of mice among groups. Five mice were initiated in the control groups (FA) and 10 in the UFP groups. One mouse died in the FA group, one in the FA+D-4F group, and two in the UFP group during the first week of subcutaneous D-4F injection. Another mouse in the UFP+D-4F group died from a wound infection due to fighting at week 8 (supplementary Table II).

### Lipid profiling

Total cholesterol was measured by enzymatic assay using a 96-well microplate-based absorbance method in accordance with the manufacturer's protocol (Thermo Trace/DMA reagent #TR13303; Fisher #NC9767174, Fisher Diagnostics, Fremont, CA; cholesterol standard 300 mg/dl Fisher #NC9343697, Thermo Scientific). HDL cholesterol was determined by employing Lipi-Direct precipitation reagent (PRDI Reference Diagnostics, Bedford, MA). Triglyceride levels were measured by using triglyceride reagent (Fisher, Infinity, catalog number TR22321) in accordance with the manufacturer's protocols. Nonfasting LDL levels were calculated using the formula: total cholesterol - HDL - triglyceride/5.

### Quantification of LDL oxidation and plasma free metabolites of arachidonic and linoleic acids

LDL was obtained by fast protein liquid chromatography (FPLC) using a Superpose 6 10/300GL column as previously described (18). Briefly, 100  $\mu\text{l}$  of plasma was applied to the column, and the samples were eluted in a mobile phase (0.15 M NaCl, 0.01% NaN<sub>3</sub>, and 2 mM EDTA, pH 7.5) at a rate of 0.3 ml/min in 30 fractions of 1.0 ml. Fractions containing LDL were extracted. The level of LDL oxidation was assessed by measuring the levels of arachidonic acid and linoleic acid metabolites including HETEs, HODEs, prostaglandin D<sub>2</sub> (PGD<sub>2</sub>), prostaglandin E<sub>2</sub> (PGE<sub>2</sub>), and thromboxane (TXB<sub>2</sub>) were determined by liquid chromatography, electron spray ionization, and tandem mass spectrometry (LC-ESI-MS/MS) as previously described (19, 20). The levels of free oxidative products of arachidonic and linoleic acids in plasma were also measured by LC-ESI-MS/MS as described (19, 20). In each instance, a deuterium-labeled internal standard was included to correct for extraction efficiency and to facilitate quantification. Extreme care was taken to prevent lipid oxidation during the analyses by including 20  $\mu\text{M}$  Butylated hydroxytoluene (BHT) and other anti-oxidants.

### Measurement of HDL oxidation index

The HDL oxidation index (HOI) was measured as an indicator of the anti-oxidant capacity of HDL that prevents LDL oxidation. The fluorescent intensity of dichlorofluorescein-diacetate (DCFH-DA) during LDL air oxidation in the presence or absence of HDL was measured as described previously (13, 21). The HOI was calculated as the ratio of dichlorofluorescein (DCF) fluorescence in the presence of HDL over the value in the absence of HDL.

### Analyses of atherosclerotic lesion size

Lesion quantification of atherosclerosis was performed in accordance with procedures described (22, 23). For en face lesion quantification of entire aortas, the aortas were dissected after perfusion-fixation, opened longitudinally from the heart to the iliac artery bifurcation, and pinned on a black wax pan for Sudan IV staining. For aortic sinus lesion quantification, the upper portion of the heart and proximal aorta was obtained, embedded in OCT compound, and stored at  $-70^{\circ}\text{C}$ . Serial 5  $\mu\text{m}$  thick cryosections of the aortic root were collected. These

sections were stained with Oil Red O. The images of the aorta and lesions were captured by using an Olympus SZX12 trinocular dissection microscope with 1× and 0.5× objectives in a blinded fashion (Olympus U-SPT and Diagnostic Instruments), 0.6× HRP060-CMT camera adapters, Q Imaging Micropublisher 5.0 RTV Digital camera, and Image Pro Plus image analysis software v4.5 (Media Cybernetics). The ratios of the area covered by atherosclerotic lesions to that of the entire aorta (en face staining) were calculated and used as lesion scores for our correlation analysis. The mean value of lipid staining areas of aortic sinus cross-sections was calculated as additional lesion score.

### Measurement of PON activity and levels of SAA and TNF- $\alpha$

PON activity was determined using paraoxon as substrate by measuring the absorbance at 412 nm in the presence of 4-nitrophenol as described (24). Briefly, the activity was measured at 25°C by adding 50  $\mu$ l of serum to 1 ml Tris-HCl buffer (100 mM at pH 8.0) containing 2 mM CaCl<sub>2</sub> and 5 mM of paraoxon. The rate of generation of 4-nitrophenol was measured at 412 nm. Enzymatic activity was computed by a molar extinction coefficient of 17,100 M<sup>-1</sup>·cm<sup>-1</sup>. Plasma SAA levels were determined by ELISA with Invitrogen's kit as previously described (25). Plasma levels of TNF- $\alpha$  were measured using ELISA kit from BioLegend following the manufacturer's instructions.

### Statistical analyses

Data were expressed as mean  $\pm$  SD. Multiple comparisons were made by one-way ANOVA, and statistical significance for pairwise comparison was determined by post hoc analyses using the Turkey test. Spearman correlation analysis was performed between lesion size and various measurements.  $P < 0.05$  was considered statistically significant.

## RESULTS

### Exposure to UFPs altered plasma lipid profiles

LDLR<sup>-/-</sup> mice fed on a HFD were exposed to FA versus UFPs for 10 weeks with or without D-4F administration (200  $\mu$ g/ml). Exposure to UFPs reduced plasma HDL levels ( $P < 0.01$ ) (Fig. 1A) and increased triglyceride levels ( $P < 0.01$ ) (Fig. 1B). The total cholesterol and calculated nonfasting LDL cholesterol levels remained statistically unchanged (supplementary Table III). Thus, exposure to UFPs reduced HDL levels, whereas administration of D-4F markedly attenuated UFP-mediated changes in HDL ( $P < 0.01$ ) and triglyceride levels ( $P < 0.05$ ) (Fig. 1).

### Exposure to UFPs reduced HDL anti-oxidant capacity and PON activity

To investigate the lipid mechanisms underlying UFP-mediated atherosclerosis, we determined HDL anti-oxidant capacity by assessing LDL oxidation. Data was expressed as a HOI using a DCF-based cell free assay (13, 21). An elevated HOI represented a decrease in HDL anti-oxidant capacity (13, 21). UFP exposure significantly increased HOI ( $P < 0.05$ ), whereas D-4F administration blocked UFP effects on HOI ( $P < 0.01$ ) (Fig. 2A).

To further assess how UFPs affected HDL anti-oxidant capacity, we quantified plasma activity of PON, a HDL-associated enzyme harboring anti-oxidant properties (22, 26). UFPs significantly reduced plasma PON activity ( $P < 0.01$ ),

whereas D-4F administration restored PON activity ( $P < 0.01$ ) (Fig. 2B). Spearman analysis further revealed a correlation between the reduction in PON activity and an increase in HOI ( $\rho = -0.72$ ,  $P < 0.01$ ) (Fig. 2C). Thus, these findings suggest that UFPs decreased HDL anti-oxidant capacity associated with reduced PON activity.

### Exposure to UFPs increased LDL oxidation and plasma levels of free HETEs and HODEs

LDL is a major risk factor of cardiovascular diseases and its oxidation is intimately associated with atherogenesis (27). We assessed LDL oxidation in mice exposed to UFPs versus FA in terms of oxidized lipid metabolites in isolated LDL. UFPs significantly increased levels of 9-HODE, 13-HODE, 5-HETE, 12-HETE, 15-HETE, 14(15)-epoxy-5Z,8Z, 11Z-eicosatrienoic acid (14-15EET), and TXB<sub>2</sub> in isolated LDL. These increases were significantly attenuated by D-4F administration (Table 1). UFP exposure did not change the levels of 20-HETE, PGD<sub>2</sub>, and PGE<sub>2</sub> in LDL (Table 1).

Oxidation products of arachidonic and linoleic acids, namely HETEs and HODEs, are intimately involved in atherogenesis (19, 28). Increased levels of these oxidation products have been associated with reduced HDL anti-oxidant capacity (13, 19). For these reasons, we measured free plasma levels of HODEs and HETEs. UFP exposure significantly increased plasma levels of 9-HODE ( $P < 0.01$ ) (Fig. 3A) and 12-HETE ( $P < 0.01$ ) (Fig. 3B). UFP exposure further engendered trends toward higher levels of 13-HODE and 5-HETE (supplementary Table IV). D-4F attenuated UFP-mediated increase in plasma 9-HODE ( $P < 0.01$ ) and 12-HETE ( $P < 0.001$ ) (Fig. 3). These findings highlighted the role of UFPs in modulating lipid metabolism.

### Exposure to UFPs increased plasma levels of SAA and TNF- $\alpha$

PM promotes inflammatory responses with relevance to the initiation of atherosclerosis (2). Akin to the C-reactive protein in humans, SAA is a systemic inflammatory marker in mice. UFP exposure significantly increased SAA levels in LDLR<sup>-/-</sup> mice ( $P < 0.01$ ), whereas D-4F attenuated UFPs increased plasma levels of SAA (Fig. 4A). PM exposure has also been reported to increase levels of inflammatory cytokines including TNF- $\alpha$  (2, 29), and to activate NF- $\kappa$ B signaling (30, 31). While UFP exposure significantly increased plasma TNF- $\alpha$  levels, D-4F did not significantly alter the levels of TNF- $\alpha$  (Fig. 4B). Hence, UFP exposure promoted systemic inflammatory responses.

### D-4F administration reduced atherosclerotic lesion scores

After 10 weeks of exposure, mouse aortas were dissected and stained with Sudan IV (en face, Fig. 5A) and Oil Red O (cross-sections of aortic sinus, Fig. 5D). UFP exposure significantly increased the en face atherosclerotic lesion ratio by 62% ( $P < 0.001$ ) (Fig. 5B) and increased the lesion area of aortic sinus sections by 220% ( $P < 0.0001$ ) (Fig. 5E). Administration of D-4F significantly reduced atherosclerotic lesion scores (Fig. 5B, E).

Spearman correlation analysis revealed that HDL levels inversely correlated with atherosclerotic lesions ( $\rho = -0.84$ ,

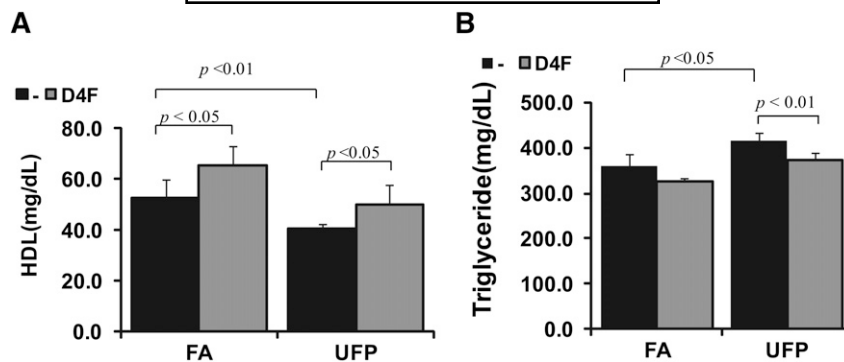


**Fig. 1.** UFP exposure modified plasma HDL and triglyceride profiles in  $LDLR^{-/-}$  mice.  $LDLR^{-/-}$  mice were exposed to FA versus UFPs for 10 weeks in the presence or absence of D-4F. Plasma levels of HDL (A) and triglyceride (B) were measured. HDL levels were significantly decreased ( $P < 0.01$ ), whereas triglyceride levels were significantly increased ( $P < 0.01$ ) in  $LDLR^{-/-}$  mice exposed to UFPs. Administration of D-4F (gray bars) significantly attenuated UFP-mediated reduction in HDL ( $P < 0.01$ ) and increase in triglyceride ( $P < 0.05$ ).

$P < 0.001$ ) (supplementary Fig. III), whereas the HOI positively correlated with lesions ( $\rho = 0.52$ ,  $P = 0.007$ ) (Fig. 5C). While the HDL levels and atherosclerotic lesions were inversely correlated in both untreated ( $\rho = -0.77$ ,  $P = 0.004$ ) and D-4F-treated mice ( $\rho = -0.80$ ,  $P = 0.001$ ) (supplementary Fig. III), the positive correlation between HOI and atherosclerotic plaque was observed in the untreated animals ( $\rho = 0.81$ ,  $P = 0.002$ ), but not in the D-4F-treated animals ( $\rho = -0.02$ ,  $P = 0.96$ ) (Fig. 5C).

PON activity was also negatively correlated with lesion ratios (supplementary Fig. IV), but D-4F did not significantly rescue this negative correlation. There were no correlations between lesion ratios and SAA levels (supplementary Fig. V) and between lesion ratios and TNF- $\alpha$  levels (supplementary Fig. VI). Thus, UFP exposure significantly increased atherosclerotic lesion ratio and area in the context of reduced HDL levels and anti-oxidant capacity.

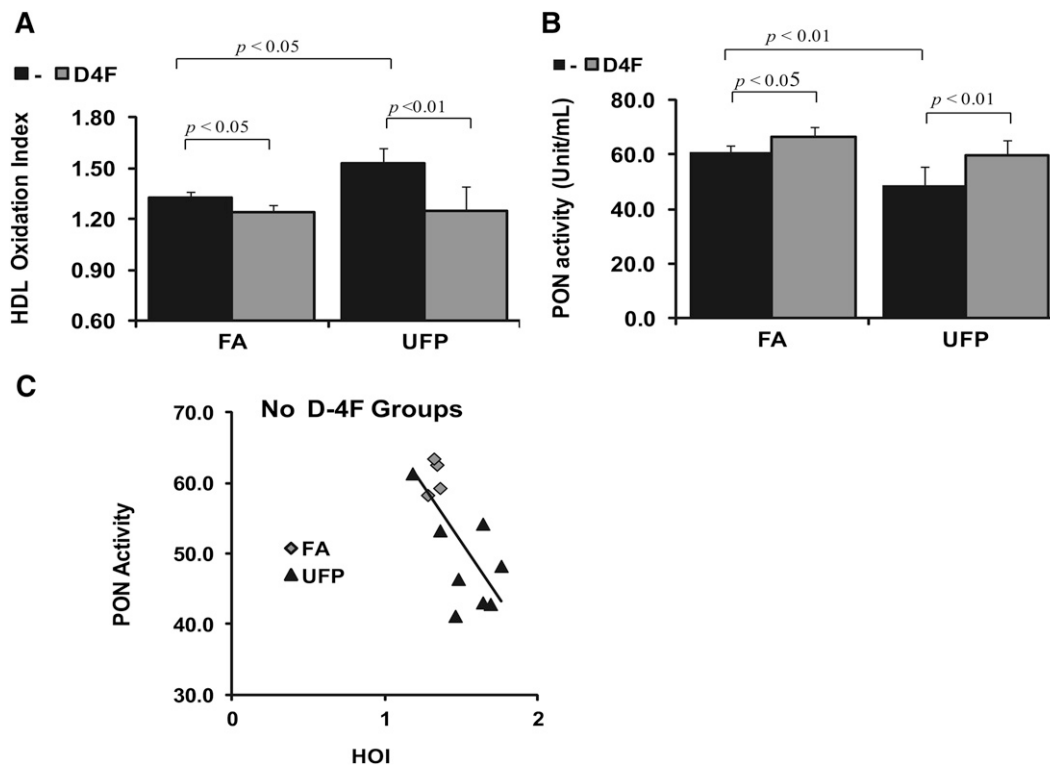


**Fig. 2.** UFPs reduced HDL anti-oxidant capacity and PON activity in  $LDLR^{-/-}$  mice. A: HOI was measured by DCF assay as a reverse indicator of HDL anti-oxidant capacity. UFPs significantly reduced HDL anti-oxidant capacity as evidenced by a significant increase in HOI (black bars). D-4F administration abrogated UFP-mediated increases in HOI (gray bars). B: Plasma PON activity was measured after 10 weeks of exposure to UFPs. UFPs significantly reduced plasma PON activity ( $P < 0.01$ ), which was restored with D-4F administration ( $P < 0.01$ ). C: Spearman correlation analysis indicated that PON activity reversely correlated with HOI ( $\rho = -0.72$ ,  $P < 0.01$ ).

TABLE 1. LDL oxidation by measurements of oxidized lipid metabolites

ng/50µg LDL	9-HODE	13-HODE	5-HETE	12-HETE	15-HETE	20-HETE	14-15EET	PGD2	PGE2	TXB2
FA	0.53 ± 0.08	5.78 ± 1.13	0.98 ± 0.14	41 ± 4.18	0.62 ± 0.07	1.31 ± 0.37	5.96 ± 0.69	0.16 ± 0.04	0.32 ± 0.07	1.45 ± 0.21
UFPs	0.74 ± 0.17 <sup>a</sup>	8.81 ± 1.07 <sup>a</sup>	1.75 ± 0.34 <sup>a</sup>	50.1 ± 6.55 <sup>a</sup>	1.01 ± 0.32 <sup>a</sup>	1.45 ± 0.37	4.57 ± 1.03 <sup>a</sup>	0.20 ± 0.07	0.42 ± 0.07	2.10 ± 0.48 <sup>a</sup>
FA+D-4F	0.32 ± 0.03 <sup>a</sup>	3.42 ± 0.85 <sup>a</sup>	0.68 ± 0.15 <sup>a</sup>	32.5 ± 2.54 <sup>a</sup>	0.46 ± 0.08 <sup>a</sup>	1.08 ± 0.25	7.65 ± 1.07 <sup>a</sup>	0.23 ± 0.07	0.31 ± 0.05	1.08 ± 0.15 <sup>a</sup>
UFPs+D-4F	0.44 ± 0.07 <sup>b</sup>	6.61 ± 1.18 <sup>b</sup>	1.30 ± 0.36 <sup>b</sup>	39.3 ± 8.51 <sup>b</sup>	0.74 ± 0.13 <sup>b</sup>	1.21 ± 0.28	5.48 ± 0.58 <sup>b</sup>	0.19 ± 0.06	0.25 ± 0.09 <sup>b</sup>	1.68 ± 0.23 <sup>b</sup>

<sup>a</sup>Versus FA, *P* < 0.05.

<sup>b</sup>Versus UFPs, *P* < 0.05.

## DISCUSSION

The current study elucidated the lipid mechanisms underlying the effects of UFP exposure to hyperlipidemic LDLR<sup>-/-</sup> mice. UFP exposure led to enhanced atherosclerotic lesions in association with UFP-mediated reduction in HDL anti-oxidant capacity and PON activities, an increase in SAA and TNF-α levels, and an increase in oxidation of LDL and lipid metabolites (HETEs and HODEs). Administration of D-4F further provided new insights into the mechanisms whereby UFPs accelerated atherosclerosis via a pro-atherogenic lipid profile and systemic inflammatory effects.

The current data performed in LDLR<sup>-/-</sup> mice recapitulated the previous study by Araujo et al. (7) in which UFP exposure to ApoE-null mice significantly increased atherosclerotic lesion size. HDL anti-inflammatory capacity was decreased by UFPs in the previous study as measured by the inhibition of HDL on monocyte binding to endothelial cells. In the current study, UFPs reduced HDL anti-oxidant capacity as measured by its ability to inhibit LDL oxidation. HDL anti-atherogenic properties include the abilities to exert anti-oxidant and anti-inflammatory actions in the vasculature (8, 9). The data from the current study are in agreement with the report revealing the anti-oxidant capacity of HDL is significantly impaired in patients with acute coronary syndromes as compared with healthy individuals or those with stable coronary artery disease (32).

Unlike the previous study (7), the current study revealed that exposure to UFPs led to a significant reduction in

HDL levels (Fig. 1A) and an increase in triglyceride levels (Fig. 1B) in LDLR<sup>-/-</sup> mice, likely due to the different genetic background (33). In addition, the concentration and duration of UFP exposure as well as diet and age of mice may have influenced the lipid profiles. In the previous study, ApoE-null mice on chow diet were exposed to concentrated ambient particles (CAPs), starting at the age of 6 weeks over a 40-day period (5 h per day, 3 days per week, for a total of 75 h). The concentration of UFPs in the exposure chamber was 5.59 (±1.23) × 10<sup>5</sup> particles/cm<sup>3</sup>. In the current study, LDLR<sup>-/-</sup> mice on a HFD were exposed to ambient UFPs at 1.91 × 10<sup>5</sup>/cm<sup>3</sup> starting at the age of 12 weeks for 5 h a day, three days a week, for 10 weeks and a total of 150 h. There were significant inverse correlations between HDL levels and atherosclerotic lesions among all animals, including untreated and D-4F-treated mice (supplementary Fig. III). D-4F treatment led to increased HDL levels and decreased atherosclerotic lesions, supporting the mechanisms by which UFPs promoted atherosclerotic lesion formation, in part, via a reduction in HDL levels in LDLR<sup>-/-</sup> mice.

UFPs also altered PON activity, plasma oxidized fatty acids, and HDL anti-oxidant capacity. Paraoxonase 1 (PON1) is an HDL-associated lactonase harboring anti-oxidant and anti-atherogenic properties (34). PON1 increases HDL binding to macrophages which, in turn, promotes HDL-mediated cholesterol efflux (34). The ability of HDL to inhibit LDL oxidation and lipid peroxidation is mediated, in part, through PON (35). Increasing evidence suggests

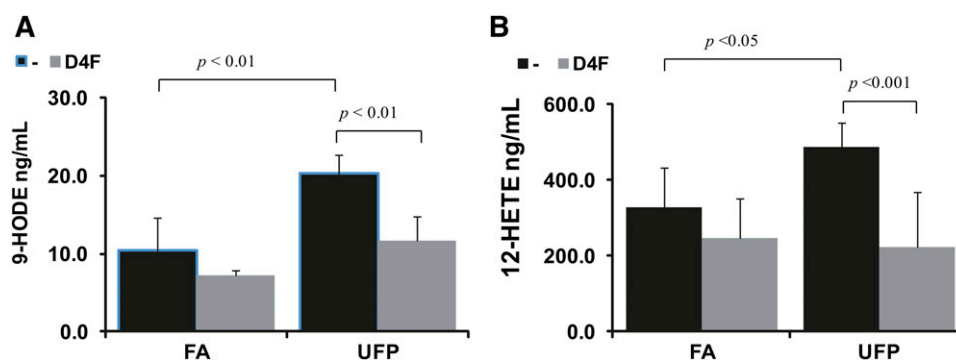


**Fig. 3.** UFPs significantly increased plasma levels of free oxidized fatty acids, 9-HODE, and 12-HETE. Plasma levels of free oxidized fatty acids (HODEs and HETEs) were analyzed by high-performance liquid chromatography, electrospray ionization, and tandem mass spectrometry (HPLC-ESI-MS/MS) after 10 weeks of UFP exposure. A: UFPs significantly increased 9-HODE levels as compared with FA (*P* < 0.01, black bars). Administration of D-4F significantly attenuated these effects (*P* < 0.01, gray bars). B: UFPs also significantly increased 12-HETE levels (*P* < 0.05, black bars), which were significantly attenuated in the presence of D-4F (*P* < 0.001, gray bars).

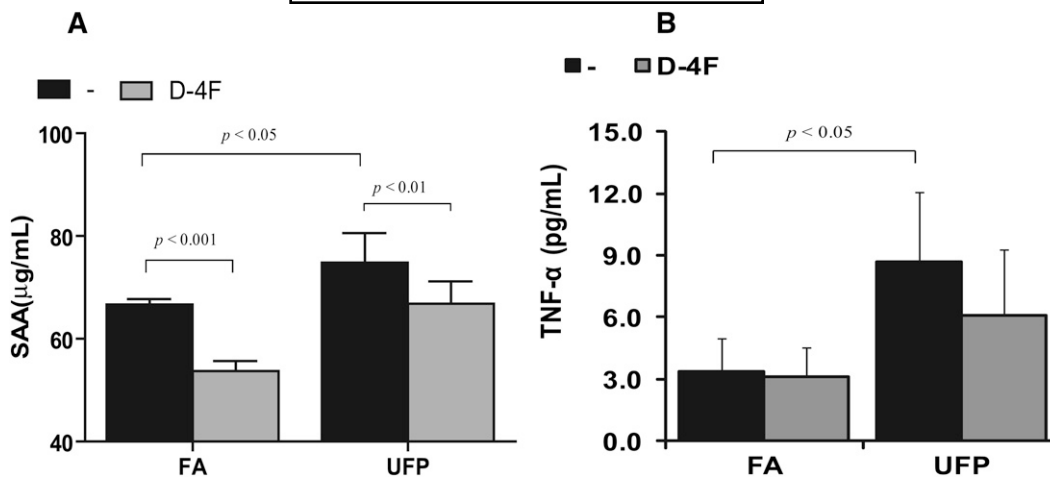


**Fig. 4.** Exposure to UFPs increased plasma levels of SAA and TNF- $\alpha$  in LDLR<sup>-/-</sup> mice. Plasma levels of SAA and TNF- $\alpha$  were measured by ELISA after 10 weeks of exposure to UFPs. UFPs significantly elevated SAA levels ( $P < 0.05$ ) and TNF- $\alpha$  levels ( $P < 0.05$ , black bars). D-4F administration attenuated UFP-mediated elevation in SAA levels ( $P < 0.01$ ) but not TNF- $\alpha$  levels (gray bars).

that PON1 mediates HDL anti-oxidant capacity to prevent LDL oxidation, as measured by a reduction in lipid peroxides (22, 26). In the current study, we observed that UFPs affected HDL anti-oxidant capacity and PON activity, and Spearman analysis corroborated a close correlation between them. Thus, a reduction in PON activity may be intimately related with an UFP-mediated decrease in HDL anti-oxidant capacity.

HDL dysfunction is associated with the pathogenesis of atherosclerosis (11, 36). HDL from diabetic patients had reduced anti-inflammatory and anti-oxidant properties, accompanied by increased free oxidized fatty acids (HETEs and HODEs) (13). Increased plasma levels of 9-HODE and 13-HODE impaired the anti-inflammatory properties of HDL (19). Here, we demonstrated that UFPs increased the plasma levels of 9-HODE and 12-HETE. While the mechanisms underlying the elevated HETE and HODE levels and reduced PON activity remain to be elucidated, removal of oxidized fatty acid from HDL was reported to restore PON activity (37). D-4F can reduce HETE and HODE plasma levels via its strong binding affinity to oxidized fatty acids (38).

The anti-oxidant activity of HDL has generated a considerable enthusiasm in HDL-based therapy. HDL and its ApoA-I can lose their protective activity to reverse transport cholesterol through changes in protein or lipid composition as well as protein modifications (7, 39). D-4F was reported to restore HDL function and to prevent diabetes-induced atherosclerosis (13). In the current study, D-4F reduced HETEs, HODEs, and the HDL oxidation index, increased PON activity, and attenuated atherosclerotic lesion size. These findings supported the notion that D-4F played an athero-protective role in UFP-exposed LDLR<sup>-/-</sup> mice, and that UFP-mediated reduction in HDL anti-oxidant capacity was implicated in the promotion of atherosclerosis. However, even though D-4F treatment fully inhibited UFP-induced changes in HDL anti-oxidant capacity, exposure to UFPs was still able to enhance atherosclerotic lesion formation among D-4F-treated mice

(Fig. 5). One possibility is that D-4F treatment may have not been able to fully normalize HDL atheroprotective properties such as anti-inflammatory capacity and reverse cholesterol transport which is supported by the fact that D-4F treatment did not completely abrogate UFP effects on SAA levels. Alternatively, UFPs may also enhance atherosclerosis via nonlipid mediated pathways as well.

The limitation of the current study lies in the small numbers of animals per treatment conditions. While UFP exposure engendered statistically significant changes such as lesion score, HDL level, anti-oxidant capacity, PON activity, etc., some of the measurements showed trends of changes consistent with lesion data but fell short by  $P$  values. For example, UFPs increased 5-HETE and 13-HODE levels, but the increases were not statistically significant ( $P = 0.18$  and  $P = 0.16$ , respectively). Similarly, D-4F treatment reduced UFP-induced TNF- $\alpha$  levels, but the  $P$  value was 0.12. Our power analysis (40) based on our current data suggests an improvement in statistical significance by increasing the number of mice to 10 in all groups in our future investigation if we are to focus on specific experimental conditions.

Overall, the strengths of the current study lie in the use of LDLR<sup>-/-</sup> mice and D-4F treatment which provide valuable insights into the mechanisms underlying UFP-mediated lipid metabolism and HDL dysfunction in close relation to atherosclerotic lesion formation. Exposure to UFPs in LDLR<sup>-/-</sup> mice recapitulated the previous finding that PM accelerated atherosclerosis in ApoE-null mice (7). In addition, the current study shows that changes in lipid metabolism and HDL functionality are likely to be pathogenic mediators in UFP-mediated atherogenesis. **RESEARCH**

The authors would like to express gratitude for the technical support from Dr. David Davis and graduate students Tyler Beebe, Karen Fang, David Mittelstein, James Hill, Katherine Quigley, and Melody Shen at USC as well as Dr. Fen Yin at University of California, Los Angeles.

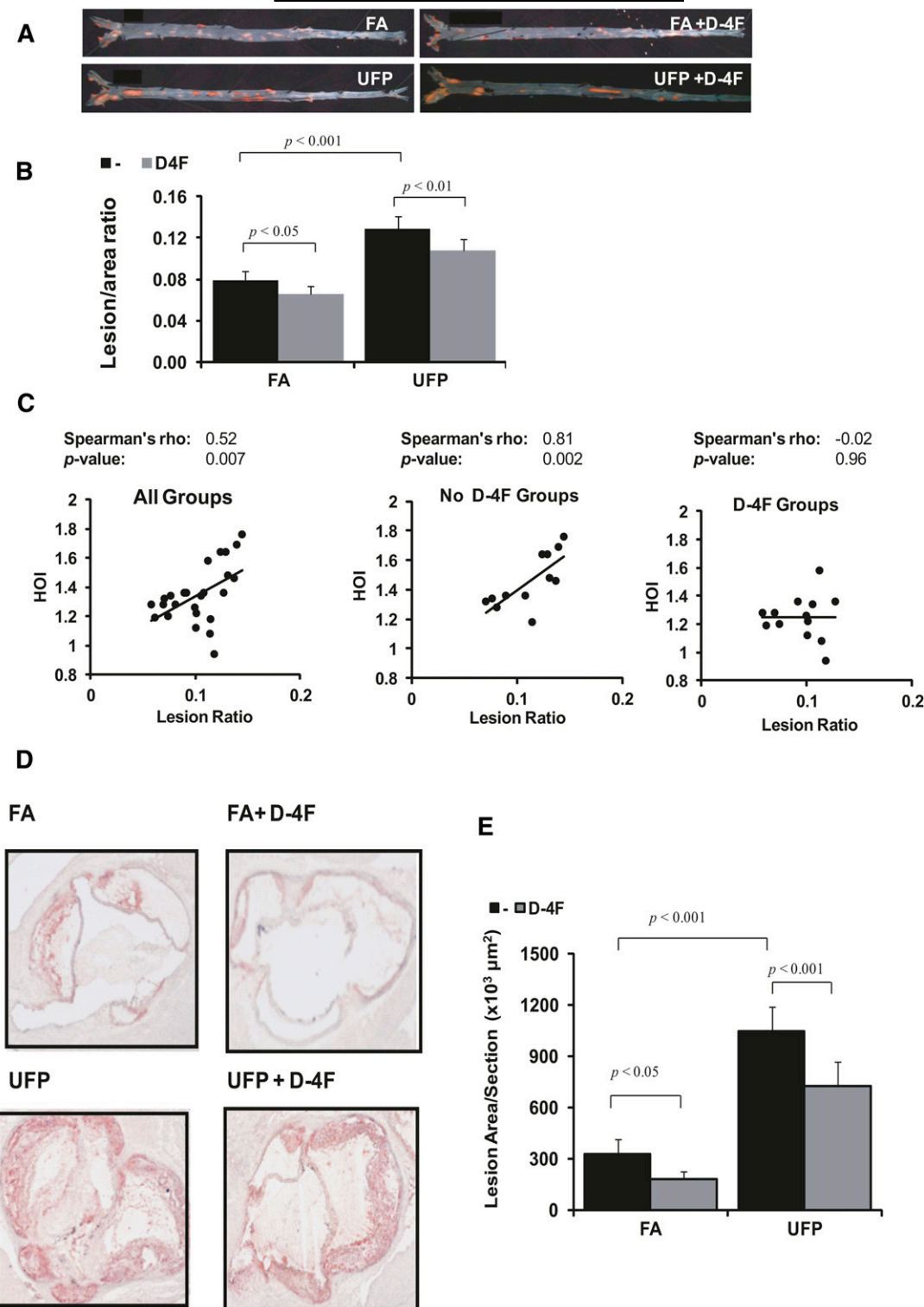


**Fig. 5.** UFP-mediated atherosclerotic lesion size correlated with a decrease in HDL anti-oxidant capacity.  $LDLR^{-/-}$  mice were exposed to FA or UFPs in the presence or absence of D-4F. **A:** En face mouse aortas were stained with Sudan IV to visualize atherosclerotic lesions (representative pictures). **B:** Atherosclerotic lesion scores were defined as the lesion/area ratios, revealing that UFPs ( $n = 8$ ,  $P < 0.001$ ) significantly increased atherosclerotic lesion size (black bars). Administration of D-4F attenuated atherosclerotic lesion size (UFPs,  $n = 9$ ,  $P < 0.01$ ) (gray bars). **C:** Correlation between UFP-mediated increase in atherosclerotic lesion size and reduction in HDL anti-oxidant capacity. Spearman analysis revealed that the HOI was positively correlated with lesion size of atherosclerosis in all mice (left panel,  $\rho = 0.52$ ,  $P < 0.007$ ) and in the absence of D-4F administration (middle panel,  $\rho = 0.81$ ,  $P < 0.002$ ). D-4F treatment led to a loss of correlation between HOI and lesion size (right panel,  $\rho = -0.02$ ,  $P = 0.96$ ), supporting the notion that D-4F reduced lesion size by restoring HDL anti-oxidant capacity. **D:** Representative pictures of atherosclerotic lesion in aortic sinus (cross-sections). **E:** Lesion quantification of aortic sinus as measured by lesion area. UFPs significantly increased lesion area ( $n = 8$ ,  $P < 0.0001$ ), which was attenuated by D-4F administration ( $n = 9$ ,  $P < 0.001$ ).

## REFERENCES

- Brook, R. D., B. Franklin, W. Cascio, Y. Hong, G. Howard, M. Lipsett, R. Luepker, M. Mittleman, J. Samet, S. C. Smith, Jr., et al. 2004. Air pollution and cardiovascular disease: a statement for healthcare professionals from the Expert Panel on Population and Prevention Science of the American Heart Association. *Circulation*. **109**: 2655–2671.
- Brook, R. D., S. Rajagopalan, C. A. Pope 3rd, J. R. Brook, A. Bhatnagar, A. V. Diez-Roux, F. Holguin, Y. Hong, R. V. Luepker, M. A. Mittleman, et al. 2010. Particulate matter air pollution and cardiovascular disease: an update to the scientific statement from the American Heart Association. *Circulation*. **121**: 2331–2378.
- Curtiss, L. K. 2009. Reversing atherosclerosis. *N. Engl. J. Med.* **360**: 1144–1146.
- Sardar, S. B., P. M. Fine, P. R. Mayo, and C. Sioutas. 2005. Size-fractionated measurements of ambient ultrafine particle chemical composition in Los Angeles using the NanoMOUDI. *Environ. Sci. Technol.* **39**: 932–944.
- Nel, A., T. Xia, L. Madler, and N. Li. 2006. Toxic potential of materials at the nanolevel. *Science*. **311**: 622–627.
- Zhang, Y., J. J. Schauer, M. M. Shafer, M. P. Hannigan, and S. J. Dutton. 2008. Source apportionment of in vitro reactive oxygen species bioassay activity from atmospheric particulate matter. *Environ. Sci. Technol.* **42**: 7502–7509.
- Araujo, J. A., B. Barajas, M. Kleinman, X. Wang, B. J. Bennett, K. W. Gong, M. Navab, J. Harkema, C. Sioutas, A. J. Lusis, et al. 2008. Ambient particulate pollutants in the ultrafine range promote early atherosclerosis and systemic oxidative stress. *Circ. Res.* **102**: 589–596.
- Navab, M., S. T. Reddy, B. J. Van Lenten, and A. M. Fogelman. 2011. HDL and cardiovascular disease: atherogenic and atheroprotective mechanisms. *Nat. Rev. Cardiol.* **8**: 222–232.
- Navab, M., R. Yu, N. Gharavi, W. Huang, N. Ezra, A. Lotfzadeh, G. M. Anantharamaiah, N. Alipour, B. J. Van Lenten, S. T. Reddy, et al. 2007. High-density lipoprotein: antioxidant and anti-inflammatory properties. *Curr. Atheroscler. Rep.* **9**: 244–248.
- Ansell, B. J., G. C. Fonarow, and A. M. Fogelman. 2007. The paradox of dysfunctional high-density lipoprotein. *Curr. Opin. Lipidol.* **18**: 427–434.
- Navab, M., S. T. Reddy, B. J. Van Lenten, G. M. Anantharamaiah, and A. M. Fogelman. 2009. The role of dysfunctional HDL in atherosclerosis. *J. Lipid Res.* **50**(Suppl.): S145–S149.
- Alwaili, K., Z. Awan, A. Alshahrani, and J. Genest. 2010. High-density lipoproteins and cardiovascular disease: 2010 update. *Expert Rev. Cardiovasc. Ther.* **8**: 413–423.
- Morgantini, C., A. Natali, B. Boldrini, S. Imaizumi, M. Navab, A. M. Fogelman, E. Ferrannini, and S. T. Reddy. 2011. Anti-inflammatory and antioxidant properties of HDLs are impaired in type 2 diabetes. *Diabetes*. **60**: 2617–2623.
- Navab, M., G. M. Anantharamaiah, S. Hama, D. W. Garber, M. Chaddha, G. Hough, R. Lallone, and A. M. Fogelman. 2002. Oral administration of an Apo A-I mimetic peptide synthesized from D-amino acids dramatically reduces atherosclerosis in mice independent of plasma cholesterol. *Circulation*. **105**: 290–292.
- Misra, C., S. Kim, S. Shen, and C. Sioutas. 2002. A high flow rate, very low pressure drop impactor for inertial separation of ultrafine from accumulation mode particles. *J. Aerosol Sci.* **33**: 735–752.
- Morgan, T. E., D. A. Davis, N. Iwata, J. A. Tanner, D. Snyder, Z. Ning, W. Kam, Y. T. Hsu, J. W. Winkler, J. C. Chen, et al. 2011. Glutamatergic neurons in rodent models respond to nanoscale particulate urban air pollutants in vivo and in vitro. *Environ. Health Perspect.* **119**: 1003–1009.
- Verma, V., Z. Ning, A. K. Cho, J. J. Schauer, M. M. Shafer, and C. Sioutas. 2009. Redox activity of urban quasi-ultrafine particles from primary and secondary sources. *Atmos. Environ.* **43**: 6360–6368.
- Jiang, X. C., L. Masucci-Magoulas, J. Mar, M. Lin, A. Walsh, J. L. Breslow, and A. Tall. 1993. Down-regulation of mRNA for the low density lipoprotein receptor in transgenic mice containing the gene for human cholesteryl ester transfer protein. Mechanism to explain accumulation of lipoprotein B particles. *J. Biol. Chem.* **268**: 27406–27412.
- Imaizumi, S., V. Grijalva, M. Navab, B. J. Van Lenten, A. C. Wagner, G. M. Anantharamaiah, A. M. Fogelman, and S. T. Reddy. 2010. L-4F differentially alters plasma levels of oxidized fatty acids resulting in more anti-inflammatory HDL in mice. *Drug Metab. Lett.* **4**: 139–148.
- Buga, G. M., M. Navab, S. Imaizumi, S. T. Reddy, B. Yekta, G. Hough, S. Chanslor, G. M. Anantharamaiah, and A. M. Fogelman. 2010. L-4F alters hyperlipidemic (but not healthy) mouse plasma to reduce platelet aggregation. *Arterioscler. Thromb. Vasc. Biol.* **30**: 283–289. [Erratum. 2010. *Arterioscler. Thromb. Vasc. Biol.* **30**: e174.]
- Navab, M., S. Y. Hama, G. P. Hough, G. Subbanagounder, S. T. Reddy, and A. M. Fogelman. 2001. A cell-free assay for detecting HDL that is dysfunctional in preventing the formation of or inactivating oxidized phospholipids. *J. Lipid Res.* **42**: 1308–1317.
- Shih, D. M., Y. R. Xia, X. P. Wang, E. Miller, L. W. Castellani, G. Subbanagounder, H. Cheroute, K. F. Faull, J. A. Berliner, J. L. Witztum, et al. 2000. Combined serum paraoxonase knockout/apolipoprotein E knockout mice exhibit increased lipoprotein oxidation and atherosclerosis. *J. Biol. Chem.* **275**: 17527–17535.
- Tangirala, R. K., E. M. Rubin, and W. Palinski. 1995. Quantitation of atherosclerosis in murine models: correlation between lesions in the aortic origin and in the entire aorta, and differences in the extent of lesions between sexes in LDL receptor-deficient and apolipoprotein E-deficient mice. *J. Lipid Res.* **36**: 2320–2328.
- Eckerson, H. W., C. M. Wyte, and B. N. La Du. 1983. The human serum paraoxonase/arylesterase polymorphism. *Am. J. Hum. Genet.* **35**: 1126–1138.
- Navab, M., S. T. Reddy, G. M. Anantharamaiah, G. Hough, G. M. Buga, J. Danciger, and A. M. Fogelman. 2012. D-4F-mediated reduction in metabolites of arachidonic and linoleic acids in the small intestine is associated with decreased inflammation in low-density lipoprotein receptor-null mice. *J. Lipid Res.* **53**: 437–445.
- Watson, A. D., J. A. Berliner, S. Y. Hama, B. N. La Du, K. F. Faull, A. M. Fogelman, and M. Navab. 1995. Protective effect of high density lipoprotein associated paraoxonase. Inhibition of the biological activity of minimally oxidized low density lipoprotein. *J. Clin. Invest.* **96**: 2882–2891.
- Peluso, I., G. Morabito, L. Urban, F. Ioannone, and M. Serafini. 2012. Oxidative stress in atherosclerosis development: the central role of LDL and oxidative burst. *Endocr. Metab. Immune Disord. Drug Targets.* **12**: 351–360.
- Funk, C. D., and T. Cyrus. 2001. 12/15-lipoxygenase, oxidative modification of LDL and atherogenesis. *Trends Cardiovasc. Med.* **11**: 116–124.
- Tsai, D. H., N. Amyai, P. Marques-Vidal, J. L. Wang, M. Riediker, V. Mooser, F. Paccaud, G. Waeber, P. Vollenweider, and M. Bochud. 2012. Effects of particulate matter on inflammatory markers in the general adult population. *Part. Fibre Toxicol.* **9**: 24.
- Li, R., D. Mittelstein, W. Kam, P. Pakbin, Y. Du, Y. Tintut, M. Navab, C. Sioutas, and T. Hsiai. 2013. Atmospheric ultrafine particles promote vascular calcification via the NF-kappaB signaling pathway. *Am. J. Physiol. Cell Physiol.* **304**: C362–C369.
- Li, R., Z. Ning, R. Majumdar, J. Cui, W. Takabe, N. Jen, C. Sioutas, and T. Hsiai. 2010. Ultrafine particles from diesel vehicle emissions at different driving cycles induce differential vascular pro-inflammatory responses: implication of chemical components and NF-kappaB signaling. *Part. Fibre Toxicol.* **7**: 6.
- Patel, P. J., A. V. Khera, K. Jafri, R. L. Wilensky, and D. J. Rader. 2011. The anti-oxidative capacity of high-density lipoprotein is reduced in acute coronary syndrome but not in stable coronary artery disease. *J. Am. Coll. Cardiol.* **58**: 2068–2075.
- Zadelaar, S., R. Kleemann, L. Verschuren, J. de Vries-Van der Weij, J. van der Hoorn, H. M. Princen, and T. Kooistra. 2007. Mouse models for atherosclerosis and pharmaceutical modifiers. *Arterioscler. Thromb. Vasc. Biol.* **27**: 1706–1721.
- Efrat, M., and M. Aviram. 2010. Paraonase 1 interactions with HDL, antioxidants and macrophages regulate atherogenesis - a protective role for HDL phospholipids. *Adv. Exp. Med. Biol.* **660**: 153–166.
- Mackness, B., and M. Mackness. 2010. Anti-inflammatory properties of paraonase-1 in atherosclerosis. *Adv. Exp. Med. Biol.* **660**: 143–151.
- Säemann, M. D., M. Poglitsch, C. Kopecky, M. Haidinger, W. H. Horl, and T. Weichhart. 2010. The versatility of HDL: a crucial anti-inflammatory regulator. *Eur. J. Clin. Invest.* **40**: 1131–1143.
- Forre, T. M., G. Subbanagounder, J. A. Berliner, P. J. Blanche, A. O. Clermont, Z. Jia, M. N. Oda, R. M. Krauss, and J. K. Bielicki. 2002. Altered activities of anti-atherogenic enzymes LCAT, paraoxonase, and platelet-activating factor acetylhydrolase in atherosclerosis-susceptible mice. *J. Lipid Res.* **43**: 477–485.
- Van Lenten, B. J., A. C. Wagner, C. L. Jung, P. Ruchala, A. J. Waring, R. I. Lehrer, A. D. Watson, S. Hama, M. Navab, G. M. Anantharamaiah, et al. 2008. Anti-inflammatory apoA-I-mimetic peptides bind oxidized lipids with much higher affinity than human apoA-I. *J. Lipid Res.* **49**: 2302–2311.
- Smith, J. D. 2010. Dysfunctional HDL as a diagnostic and therapeutic target. *Arterioscler. Thromb. Vasc. Biol.* **30**: 151–155.
- Snedecor, G. W., and W. G. Cochran. 1989. *Statistical Methods*. 8th edition. Iowa State University Press, Ames, Iowa.